Variational Methods in the pursuit of an Action Principle in Fluid Turbulence

Rich Kerswell

Mathematics

Bristol University

- Malkus' original idea – Maximum Entropy Production
- Variational Techniques

  a) Euler-Lagrange (Howard-Busse)

  b) Background approach (Doering-Constantin)
- "Efficiency" functional

Rayleigh-Benard convection

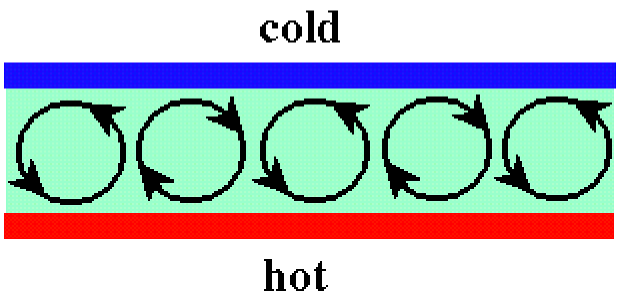

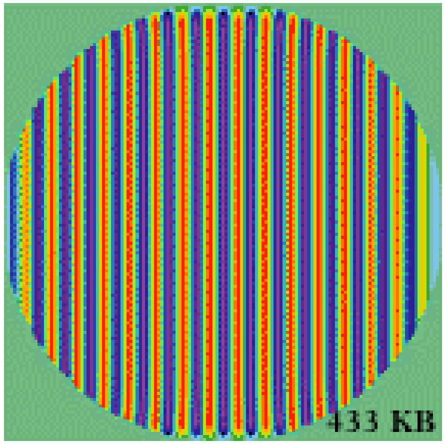

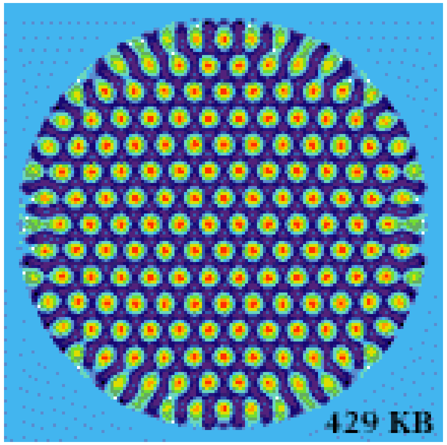

Malkus (1954a,b)

``Of all the possible solutions, the one which is selected is that which has the largest heat transport''

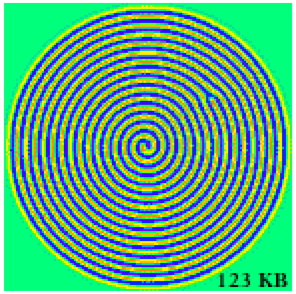

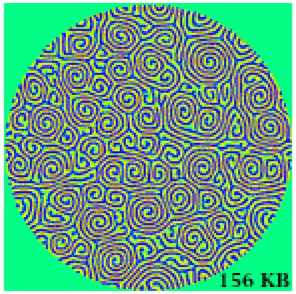

Malkus & Veronis (1958)

Extend competition to non-solutions - Howard (1963)

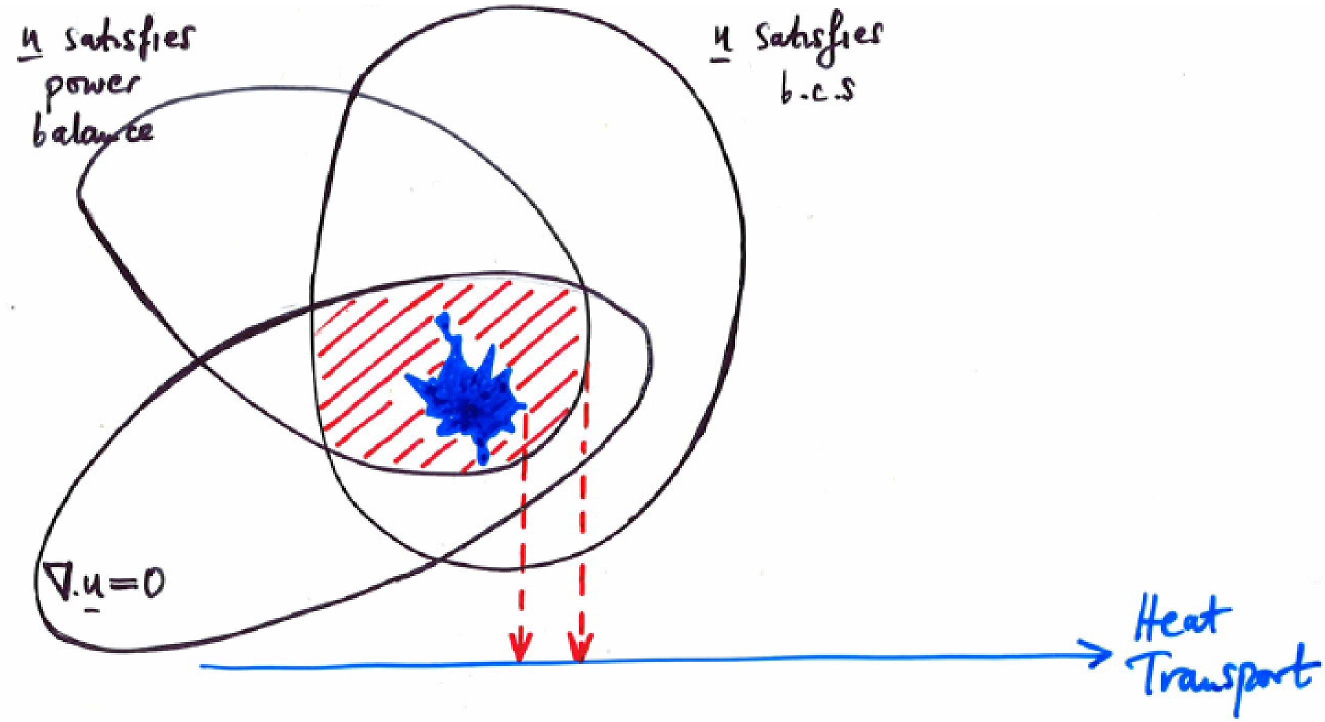

— strict upper bound

— applicable to turbulence

Classical Variational Approach

Busse (1970)

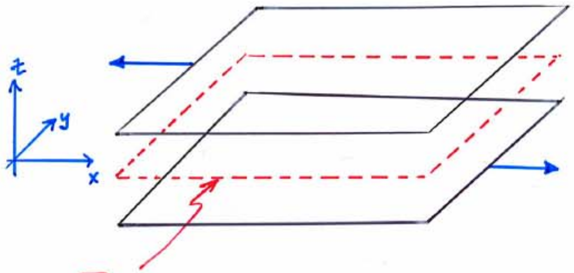

$$\frac{\partial \underline{u}}{\partial t} + \underline{u}.\nabla\underline{u} + \nabla p = \nabla^2\underline{u}$$

$$\nabla.\underline{u} = 0$$

$$\underline{u} = \pm\tfrac{1}{2}Re\,\hat{\underline{x}} \quad z = \mp\tfrac{1}{2}$$

$$Re := \frac{V_0 d}{\nu}$$

$\overline{(\ )} \equiv$ averaging over z planes

$\langle\ \rangle \equiv \int dV$

Assumptions
- $\underline{u}(\underline{x},t) = U(z)\hat{\underline{x}} + \underline{v}(\underline{x},t)$ with $\overline{\underline{v}} = \underline{0}$ so $\frac{\partial}{\partial t}\overline{\underline{u}} = \underline{0}$
- $\frac{d}{dt}\langle\tfrac{1}{2}\underline{v}^2\rangle = 0$ on 'average' — Statistical Stationarity

Problem: maximize $D = \int |\nabla\underline{u}|^2 dV$

subject to

i) total power balance $\int \underline{u}.\left[\frac{\partial\underline{u}}{\partial t} + \underline{u}.\nabla\underline{u} + \nabla p - \nabla^2\underline{u}\right] d\underline{x} = 0$

$$\Rightarrow \langle U'^2 + |\nabla\times\underline{v}|^2\rangle = -Re\left.\frac{dU}{dz}\right|_{\partial V} = Re^2 + Re\langle uw\rangle$$

ii) mean momentum balance in $\hat{\underline{x}}$ direction

$$\lim_{L\to\infty}\frac{1}{4L^2}\int_{-L}^{L}dx\int_{-L}^{L}dy\ \hat{\underline{x}}.\left[\frac{\partial\underline{u}}{\partial t} + \underline{u}.\nabla\underline{u} + \nabla p - \nabla^2\underline{u}\right] = 0$$

$$\Rightarrow \frac{dU}{dz} = \overline{uw} - \langle uw\rangle - Re$$

iii) flow incompressible $\nabla.\underline{u} = 0$

iv) $\underline{u}$ satisfies b.c.s $\underline{u}(x,y,\mp\tfrac{1}{2}) = \pm\tfrac{1}{2}Re\,\hat{\underline{x}}$

Euler–Lagrange Eq$^{\underline{n}}$

$$\Rightarrow \left[\overline{uw} - \langle uw\rangle - \frac{Re}{2} - \frac{\langle(\overline{uw} - \langle uw\rangle)^2\rangle}{2\langle uw\rangle}\right]\begin{bmatrix} w \\ 0 \\ u \end{bmatrix} + \nabla p = \nabla^2\underline{v}$$

$$\nabla.\underline{v} = 0$$

$$\underline{v}(x,y,\pm\tfrac{1}{2}) = 0$$

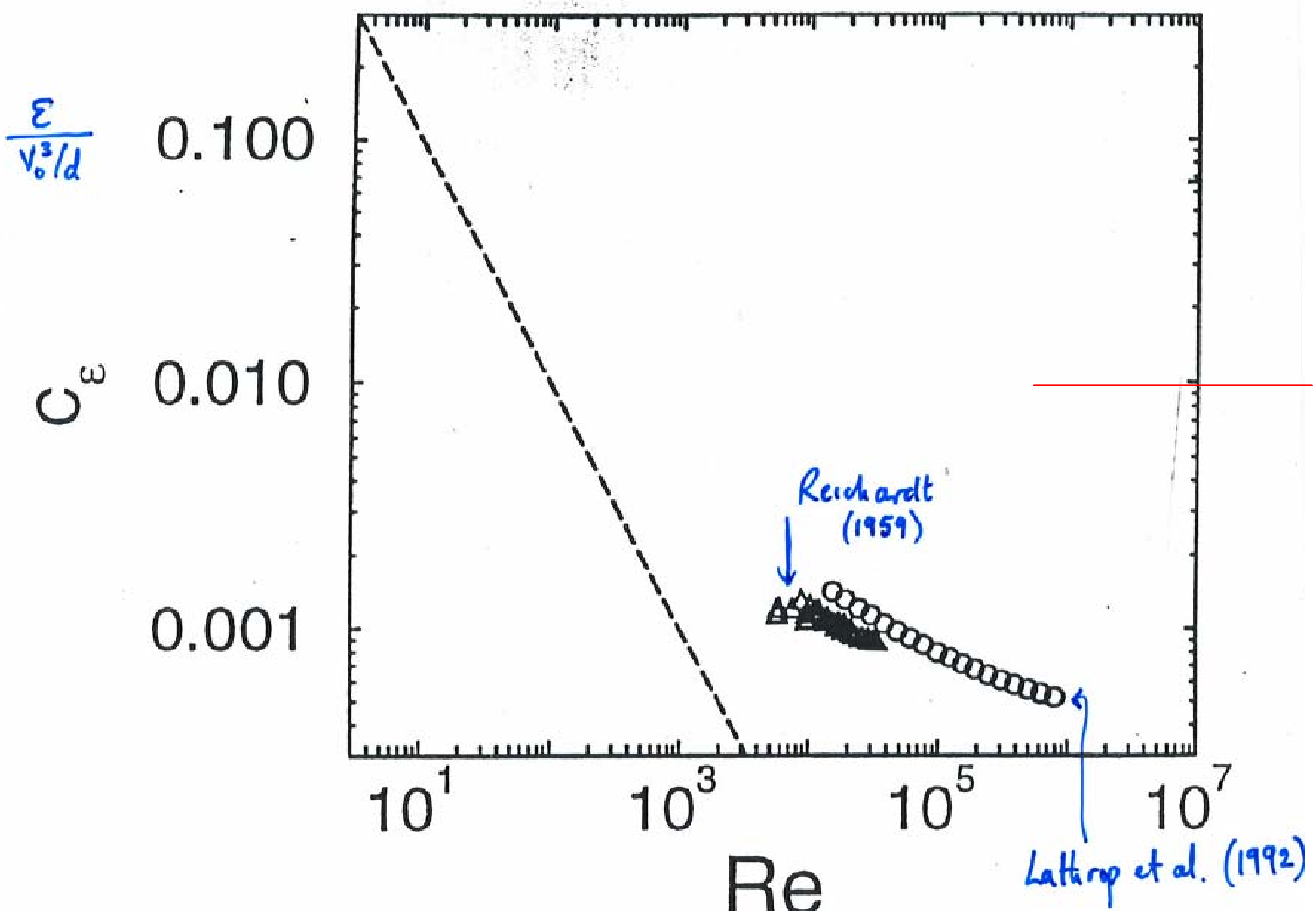

$\frac{\varepsilon}{V_0^3/d}$
0.100
C^{ε}
0.010
0.001
Reichardt (1959)
10^1
10^3
10^5
10^7
Re
Lathrop et al. (1992)

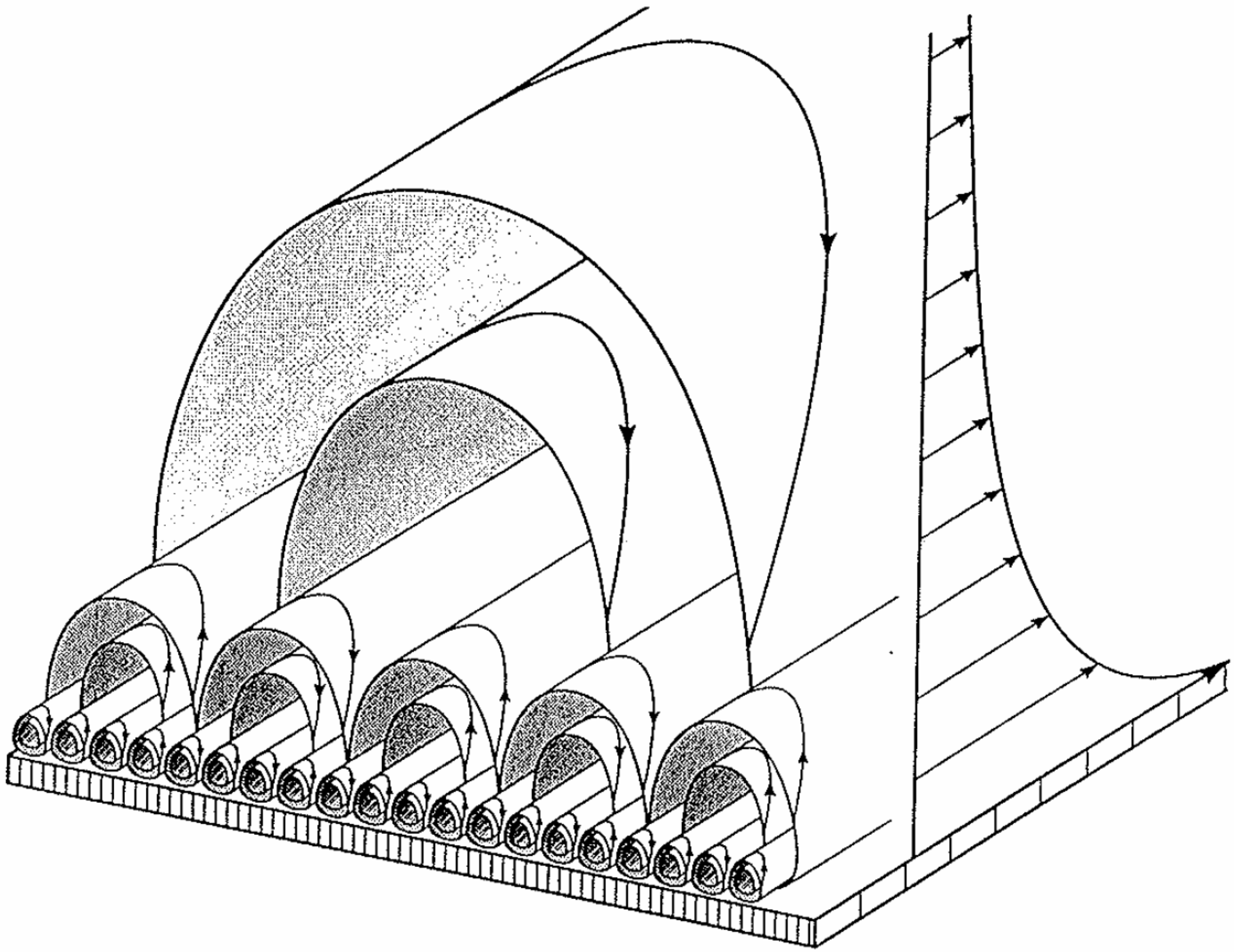

Fig. 1. Qualitative sketch of the nested boundary layers which characterize the vector field of maximum transport.

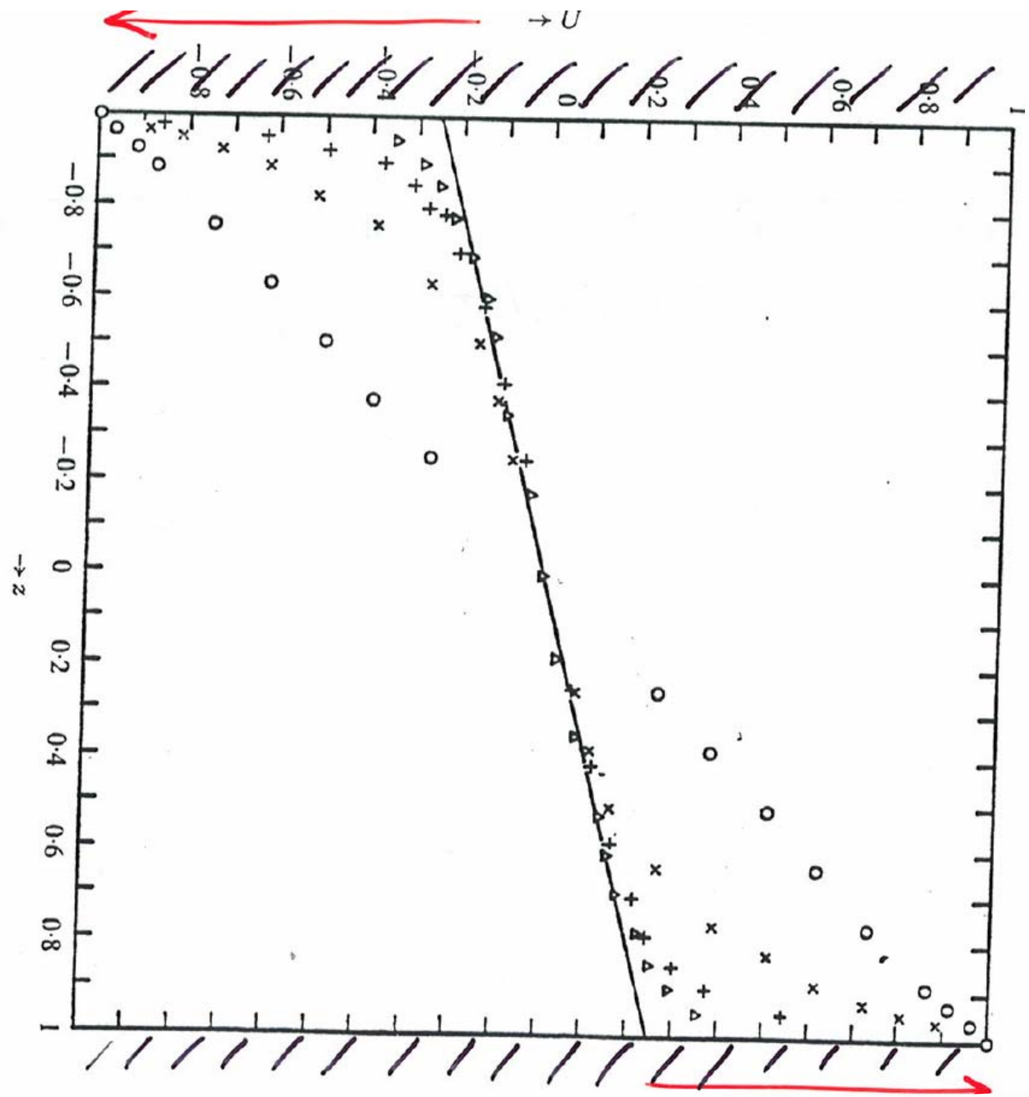

FIGURE 2. The mean velocity in plane Couette flow measured by Reichardt (1959) at $Re = 1200$ (○), $Re = 2900$ (×), $Re = 5900$ (+), and $Re = 34000$ (△). The straight line describes the asymptotic profile corresponding to the extremalizing solution of the variational problem.

Busse 1970

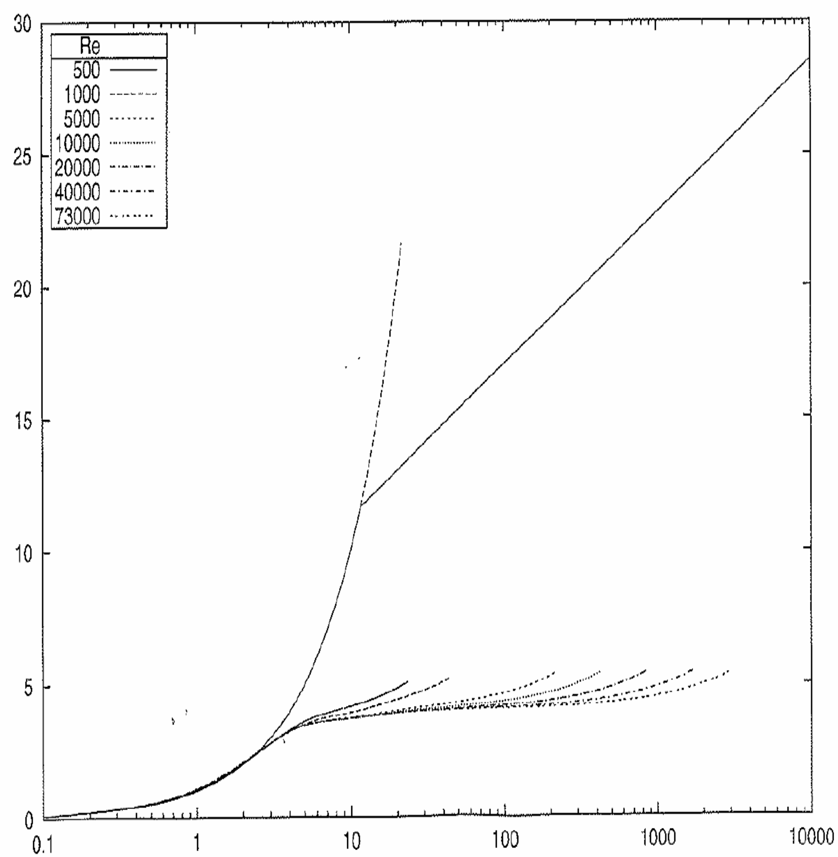

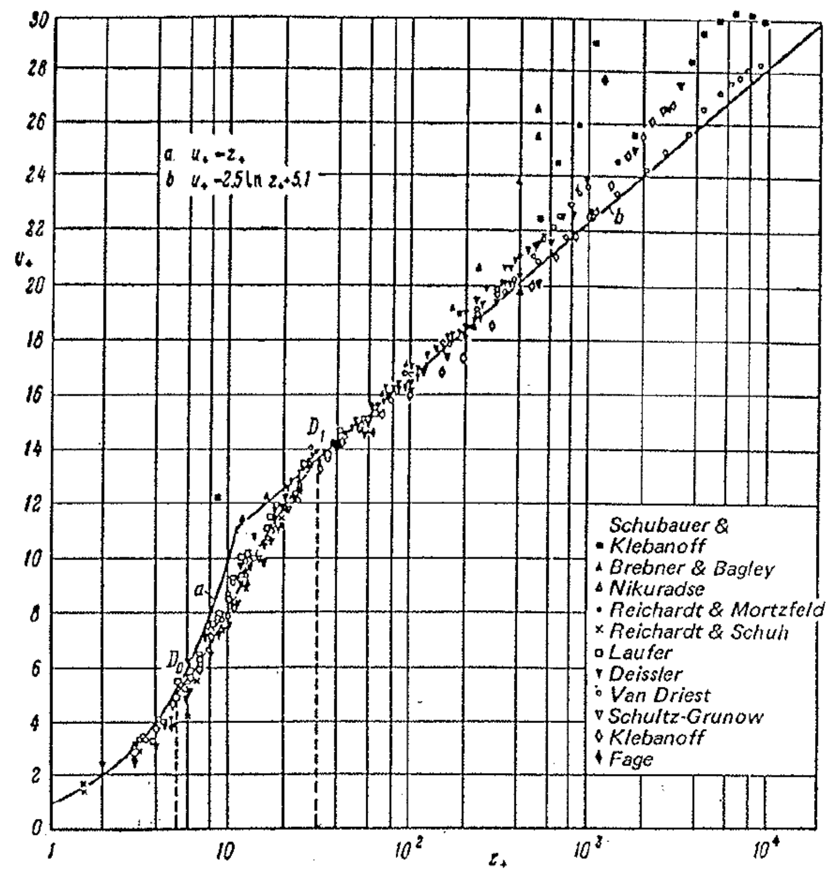

FIG. 25. Universal dimensionless mean velocity profile of turbulent flow close to a smooth wall according to the data of tube-, channel- and boundary-layer measurements [according to Kestin and Richardson (1963)].

Plasting & K 2003

Doering & Constantin (1992, 1994, 1995, 1996)
(Nicodemus et al. 1997)

$$\underline{u}(\underline{x},t) = \phi(z)\hat{\underline{x}} + \underline{v}(\underline{x},t)$$

(Hopf 1941)

'Background' field
$\phi(\pm\frac{1}{2}) = \mp\frac{1}{2}Re$

'Fluctuations'
$\underline{v} = \underline{0}|_{\partial V}$; $\overline{\underline{v}} \neq \underline{0}$

Physical Information

$$\int \underline{v}\cdot\left[\frac{\partial \underline{u}}{\partial t} + \underline{u}.\nabla\underline{u} + \nabla p - \nabla^2\underline{u}\right] d\underline{x} = 0$$

$$\Rightarrow \frac{\partial}{\partial t}\int \tfrac{1}{2}\underline{v}^2\, d\underline{x} = \int \phi'' v_1 - |\nabla\underline{v}|^2 - \phi' v_1 v_3\, d\underline{x} \qquad (\mathrm{I})$$

Identity $\quad Re^3 D = \int |\nabla\underline{u}|^2 d\underline{x} = \int |\phi'\hat{\underline{x}} + \nabla\underline{v}|^2 d\underline{x}$

$$= \int \phi'^2 - 2\phi'' v_1 + |\nabla\underline{v}|^2\, d\underline{x} \qquad (\mathrm{II})$$

$(\mathrm{II}) + a(\mathrm{I}) \Rightarrow$

$$Re^3 D + a\frac{\partial}{\partial t}\int \tfrac{1}{2}\underline{v}^2 d\underline{x} = \int \phi'^2 - 2\phi'' v_1 + |\nabla\underline{v}|^2 + a\phi'' v_1 - a|\nabla\underline{v}|^2 - a\phi' v_1 v_3\, d\underline{x}$$

Take long time averages $\left(\lim_{T\to\infty} \frac{1}{T}\int_0^T \frac{\partial}{\partial t}\int \tfrac{1}{2}\underline{v}^2 d\underline{x}\ dt = 0 \right)$

$$\lim_{T\to\infty}\frac{1}{T}\int_0^T Re^3 D\, dt = \int \phi'^2 d\underline{x} - \lim_{T\to\infty}\frac{1}{T}\int_0^T dt \int (a-1)|\nabla\underline{v}|^2 + a\phi' v_1 v_3 - (a-2)\phi'' v_1\, d\underline{x}$$

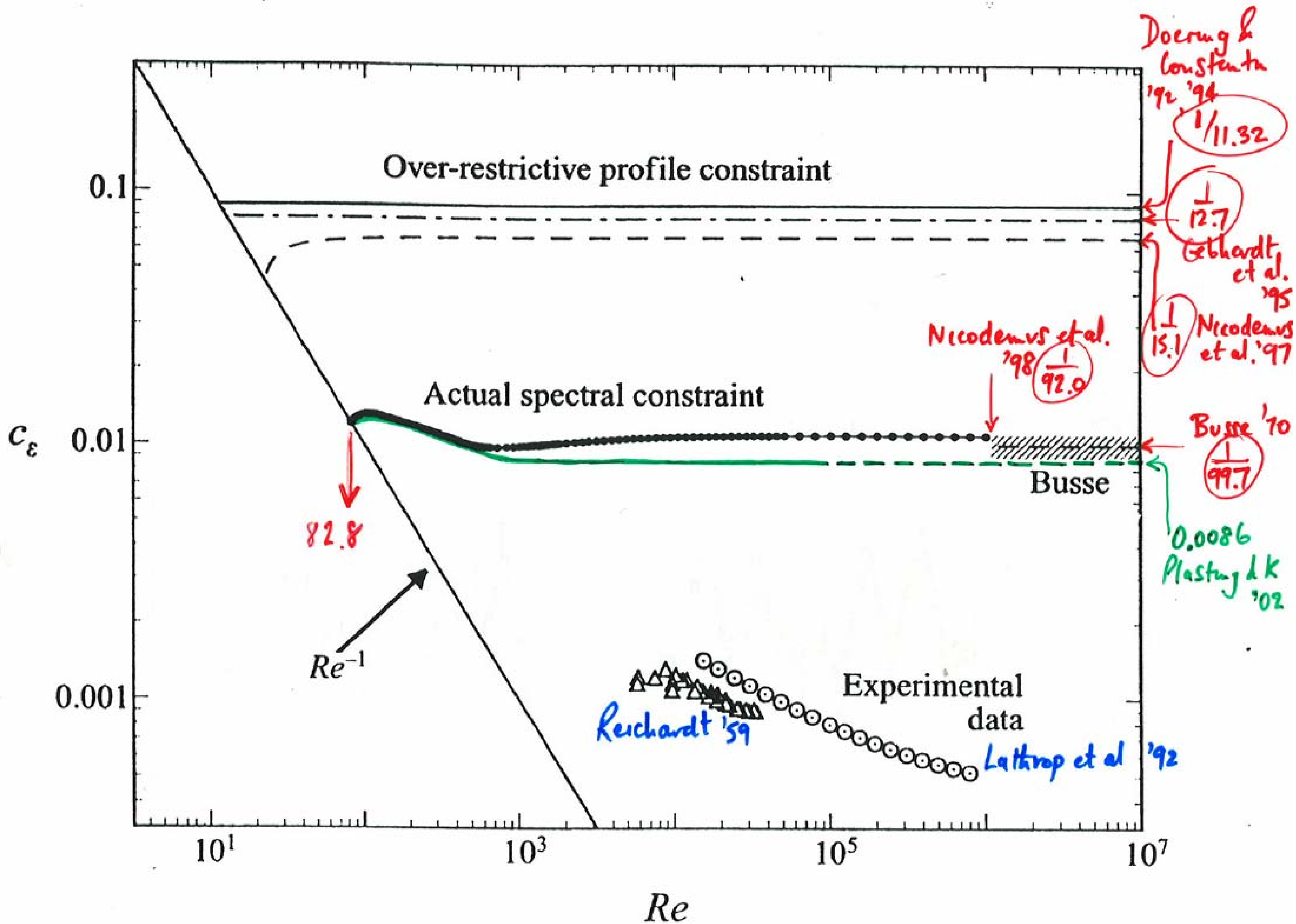

Over-restrictive profile constraint
Actual spectral constraint
Busse
Experimental data
Re^{-1}
c_ε
Re
0.1
0.01
0.001
10^1
10^3
10^5
10^7
Doering & Constantin '92, '94
1/11.32
1/12.7
Gebhardt et al. '95
1/15.1
Nicodemus et al. '97
Nicodemus et al. '98
1/92.9
Busse '70
1/99.7
0.0086
Plasting & K '02
82.8
Reichardt '59
Lathrop et al '92

$$\max/\min \ u^2 \quad \text{s.t.} \quad u = 1$$

$$\mathcal{L} = u^2 - av(u-1)$$

define $\phi = u - v$

$$\Rightarrow \mathcal{L} = \phi^2 + (2-a)v\phi - (a-1)v^2 + av$$

(a) $\left.\frac{\partial \mathcal{L}}{\partial v}\right|_{\phi} = 0 \Rightarrow v = \frac{(2-a)\phi + a}{2(a-1)}$

$$\Rightarrow \mathcal{L} = 1 + \frac{[a\phi + (2-a)]^2}{4(a-1)}$$

MINIMIZATION problem over ϕ (D–C)

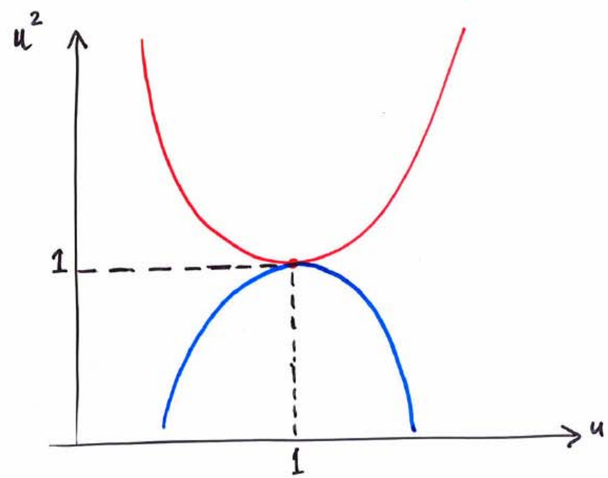

(b) $\left.\frac{\partial \mathcal{L}}{\partial \phi}\right|_{v} = 0 \Rightarrow \phi = \left(\frac{a-2}{2}\right)v$

$$\Rightarrow \mathcal{L} = 1 - \left(\frac{a}{2}v - 1\right)^2$$

MAXIMIZATION problem over v (B)

Stability of the Mean Profile?

parametrization of data (Reynolds & Tiederman 1967)

$$U(y) = RB \int_0^y \frac{1-y'}{1+E(y')}\,\mathrm{d}y', \tag{3.1}$$

where
$$R = \frac{\langle U \rangle y_0}{\nu}, \quad B = -\frac{\partial P}{\partial x}(y=0), \quad \int_0^1 U\,\mathrm{d}y = 1, \tag{3.2}$$

and
$$E(y) = \frac{1}{2}\left\{1 + \frac{K^2R^2B}{9}(2y-y^2)^2(3-4y+2y^2)^2\left(1-\exp\frac{-yRB^{\frac{1}{2}}}{A}\right)^2\right\}^{\frac{1}{2}} - \tfrac{1}{2}. \tag{3.3}$$

(A) Linear Stability of $U(y)$ Reynolds & Tiederman (1967)

$Re^* \simeq 10\,Re$

(B) Linear Stability of $U(y)$ + Reynolds Stress component of OS mode

$Re^* \simeq 5\,Re$

(C) Linear Stability of $U(y)\hat{\underline{x}} + A^* \underline{u}_{OS}^{2D}$ to 3D disturbances

Ierley & Malkus (1988)

$Re^* \sim Re$ of A^* such that u_{OS}^{2D} peak speed is 25% local mean velocity

$\ll$ that required to make mean inflexional

100% = 1% energy of mean

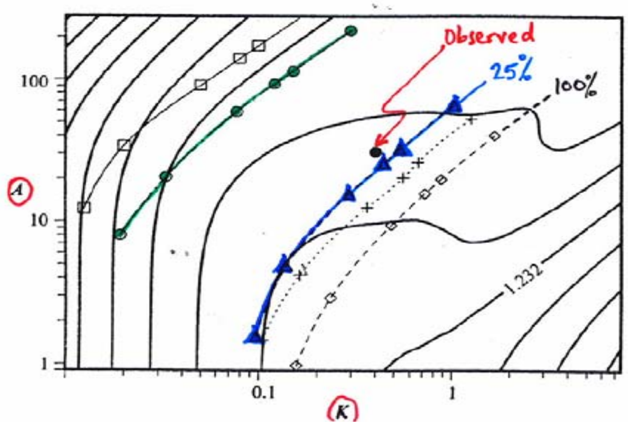

Alternative functionals

Malkus & Smith (1989) PPF
Smith (1991) PCF
Ierley & Worthing (2001) HPF

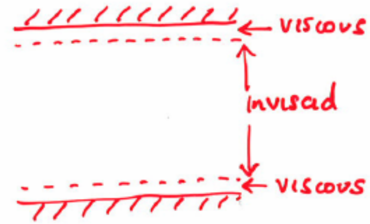

'Approximate' Variational Problem

$$\max \; f = D \times I^n \qquad I := \frac{D_{\text{fluctuation}}}{D_{\text{mean}}} = \frac{D_v}{D_m}$$

over all $u^+(z)$ where

a) smallest scale of motion in $u^+(z)$ is given by a critical boundary Reynolds number

b) 'Interior' is inviscidly stable $u^{+''} < 0$

c) b.c.s implied on u^+ via mean momentum balance

$$u^{+'''} = u^+ = 0 \; ; \; u^{+''} = R^* \; ; \; u^{+'} = \pm R^* \quad \text{at } z = \mp 1$$

$$u^{+''} = -I^* I \quad \text{where } I = \sum_{0}^{k_0} I_k e^{ik(1+z)\pi} \quad (\text{Fejér})$$

$n = 1$ gives interesting results

christened $f = DI$ the "efficiency" functional

Efficiency
$\mathcal{E}_1 = \mathcal{E}\left(\frac{\mathcal{E}_{fluct}}{\mathcal{E}_{mean}}\right)$

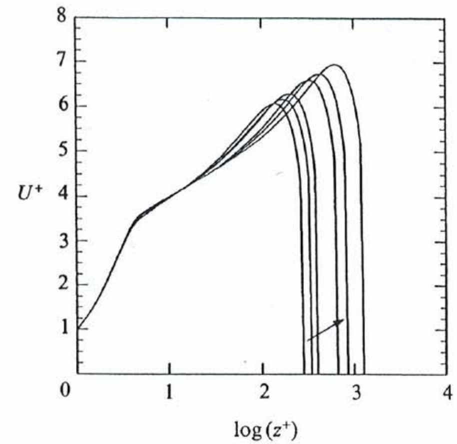

FIGURE 9. Maximum-$\mathscr{E}$ profiles for $R = 738$, 922, 1107 (numerical) and $R = 1913$, 2519, 3867 (approximate). $k_0 = 89$, 109, 128, 210, 270, 400.

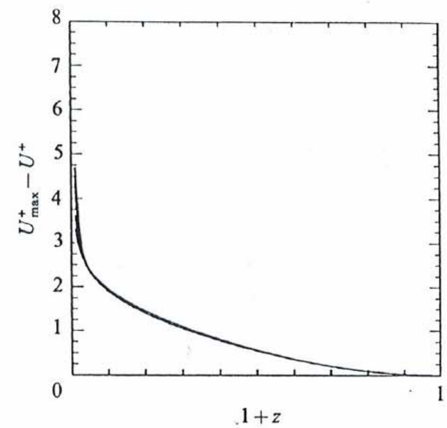

FIGURE 10. Maximum-$\mathscr{E}$ velocity defect law of both the numerical and approximate profiles.

Malkus & Smith (1989)

e.g. Plane Poiseuille Flow (PPF)

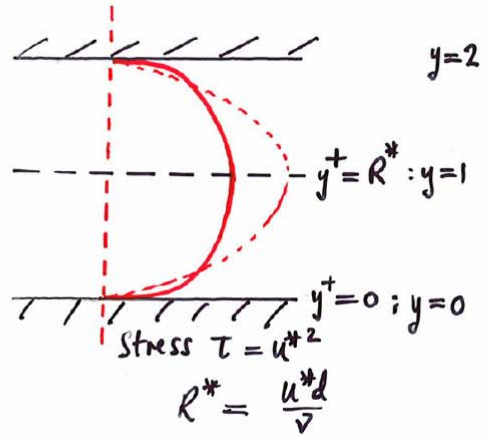

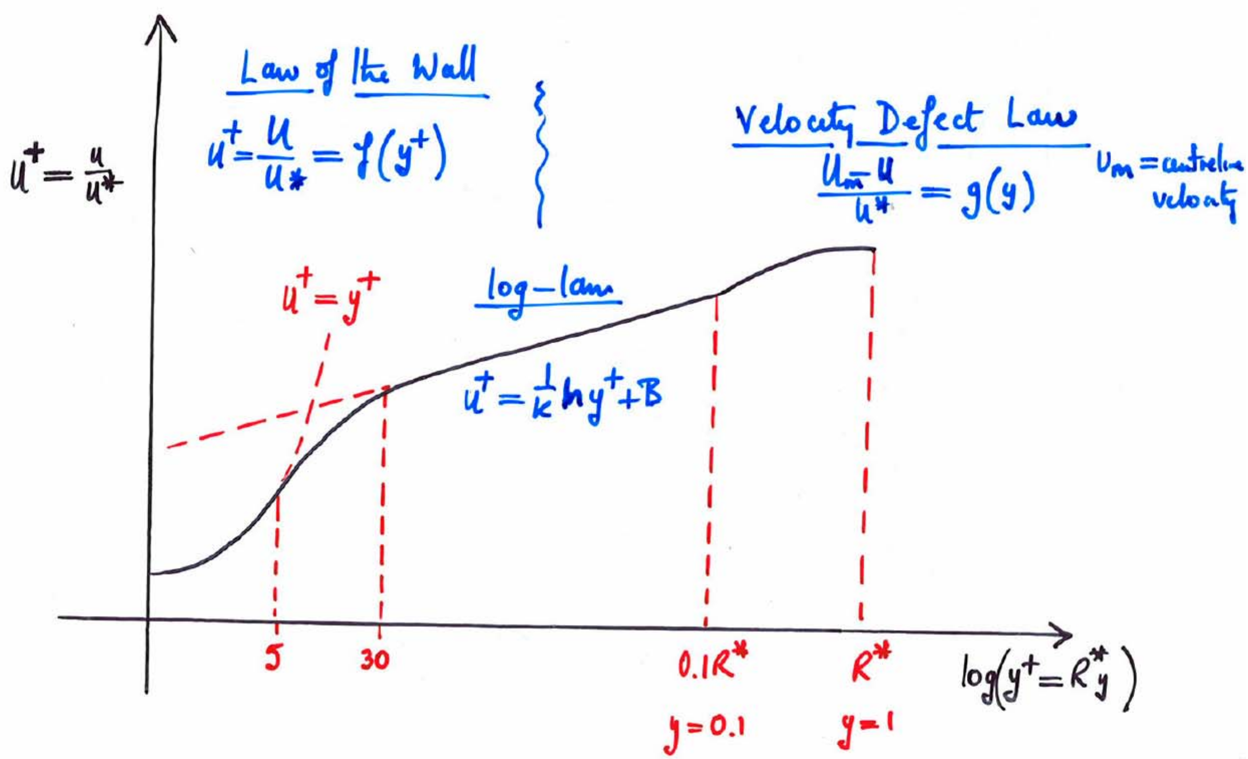

Malkus & Smith (1989)

Mean fields

data & optimal sol!

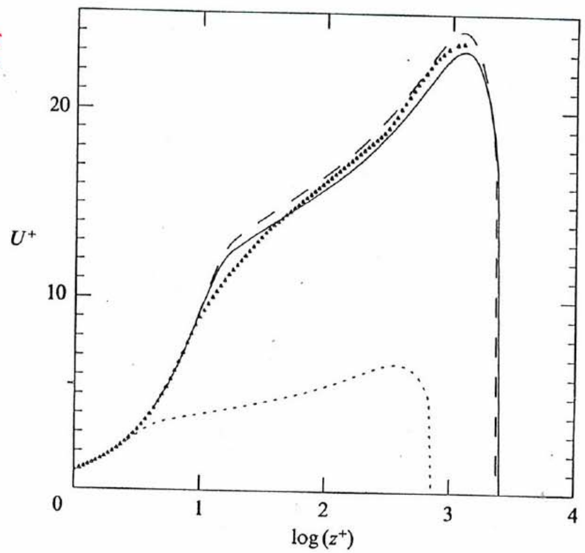

FIGURE 12. Recent experimental data for Poiseuille channel flow, and $\mathscr{E}$ upper-bound profiles : different R_c. $\triangle$, data (Johansson *et al.* 1983), for $R \approx 25600$; ——, maximum-$\mathscr{E}$ profile with R_c 480 ($k_0 = 230$, $R \approx 25600$); ——, maximum-$\mathscr{E}$ profile with $R_c = 529$ ($k_0 = 210$, $R \approx 25600$); -- maximum-$\mathscr{E}$ profile with $R_c = 39.69$ ($k_0 = 230$, $R \approx 2100$).

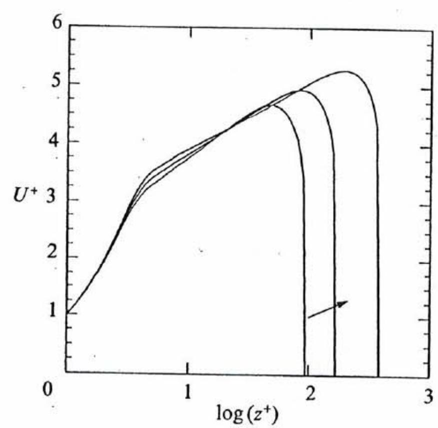

FIGURE 13. Maximum-$R^{\frac{5}{2}}_{\frac{7}{7}}I$ profiles for $R = 192$, 369, 1107 ($k_0 = 30$, 53, 121).

Apply variational machinery to "efficiency" functional

$$f = D I^n \quad \& \quad D_m I^n$$

in plane Couette flow (PCF)
& plane Poiseuille flow (PPF) (K 2002)

Results

f		I	D	(PCF) interior shear
DI^n	$0 \leq n < 1$	$O(1)$	$O(Re^3)$	$-\left(\frac{3n+1}{4}\right) Re$
"efficiency"	$n = 1$	$O(Re^{\frac{1}{3}})$	$O(Re^{8/3})$	$-Re$ (laminar)
	$n > 1$	$O(Re^{\frac{1}{2}})$	$O(Re^{5/2})$	$-Re$
D_m		$\frac{1}{2}$	$O(Re^3)$	0
Observed (Prandtl–von Kármán)		$O(\log Re)$	$O\left(\frac{Re^3}{(\log Re)^2}\right)$	0 (presumed as $Re \to \infty$)

- Efficiency does not give a log-layer & velocity defect law
- D_m gives correct interior for PCF but incorrect for PPF
- 'stability' missing!

Summary

Variational methods are a valuable tool

- Extract (inequality) scaling laws

  e.g. wall-bounded shear flows $e \sim O(1)$ as $n \to 0$

  Boussinesq convection $Nu \sim Ra^{1/2}$

- Test hypotheses

  (a) effect of extra constraints…

  (b) look for an Action functional

  - Efficiency is promising but unsubstantiated

    Key omissions are Stability constraints…

Theorem

In Plane Couette flow, for a velocity field which satisfies the Navier–Stokes equations & the smoothness constraint that the minimum lengthscale parallel to the plates $\geq \lambda Re^{2\alpha-1}$ then the energy dissipation rate $\varepsilon \leqslant \varepsilon_{bound}$ where

$$\frac{0.308}{\sqrt{\lambda}} Re^{-\alpha} \leqslant \varepsilon_{bound} \leqslant \frac{0.562}{\sqrt{\lambda}} Re^{-\alpha} \qquad \text{as } Re \to \infty$$

(Kerswell 2000)

Implications

1. If $\varepsilon \sim O(1)$ (or there are logarithmic corrections)

   $\Rightarrow$ transverse lengthscales down to $O(Re^{-1})$ are important

2. Numerical simulations which adopt, e.g, $|k|_{max} = \dfrac{2\pi}{\ell_{kolmogorov}}$ will manage at best $\varepsilon \sim Re^{-1/7}$

3. Suggests numerical experiments in which transverse scales are artificially restricted.

(PPF) Plane Poiseuille Flow

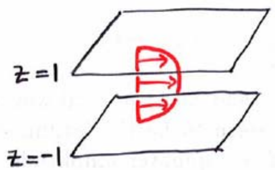

$$\underline{V} = \sum_{\underline{k}}{}' \, \underline{v}_{\underline{k}}(z,t)\, e^{i\underline{k}\cdot\underline{x}}$$

$$\underline{k} = (k_1, k_2, 0)$$

$$-10 \leq k_1, k_2 \leq 10$$

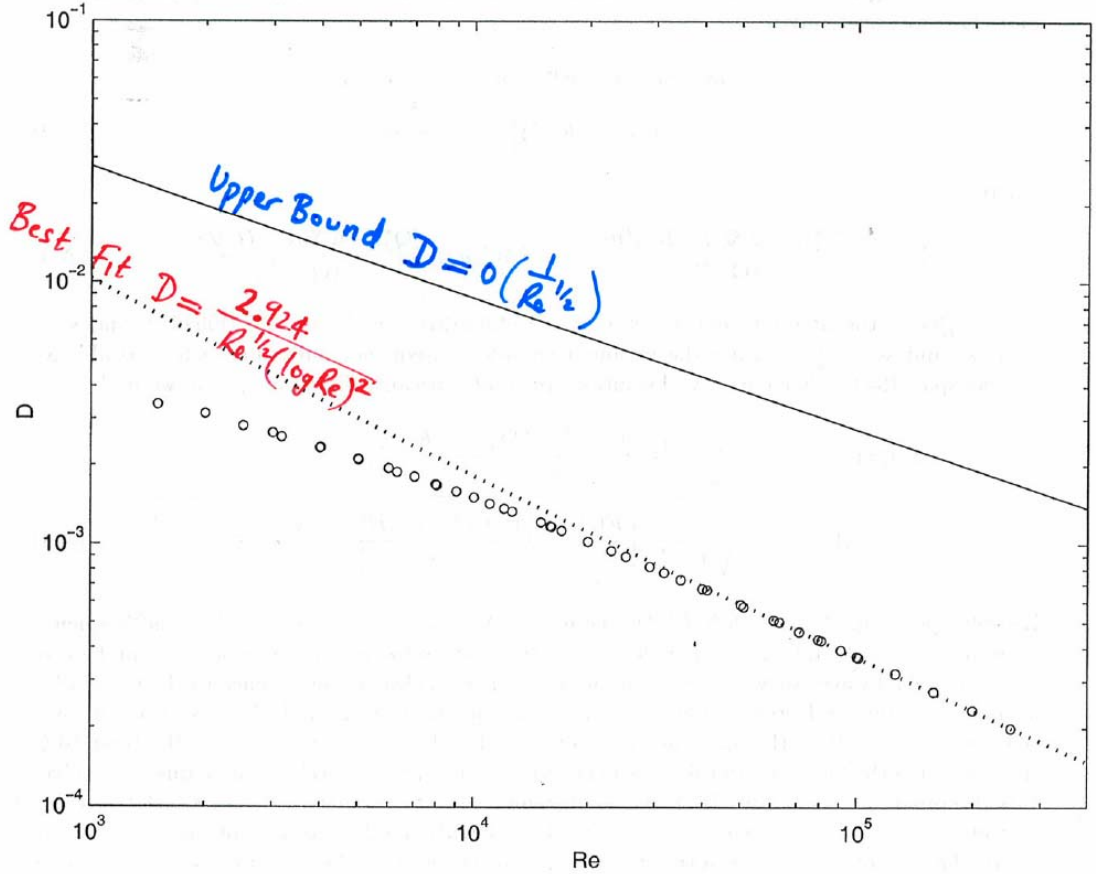

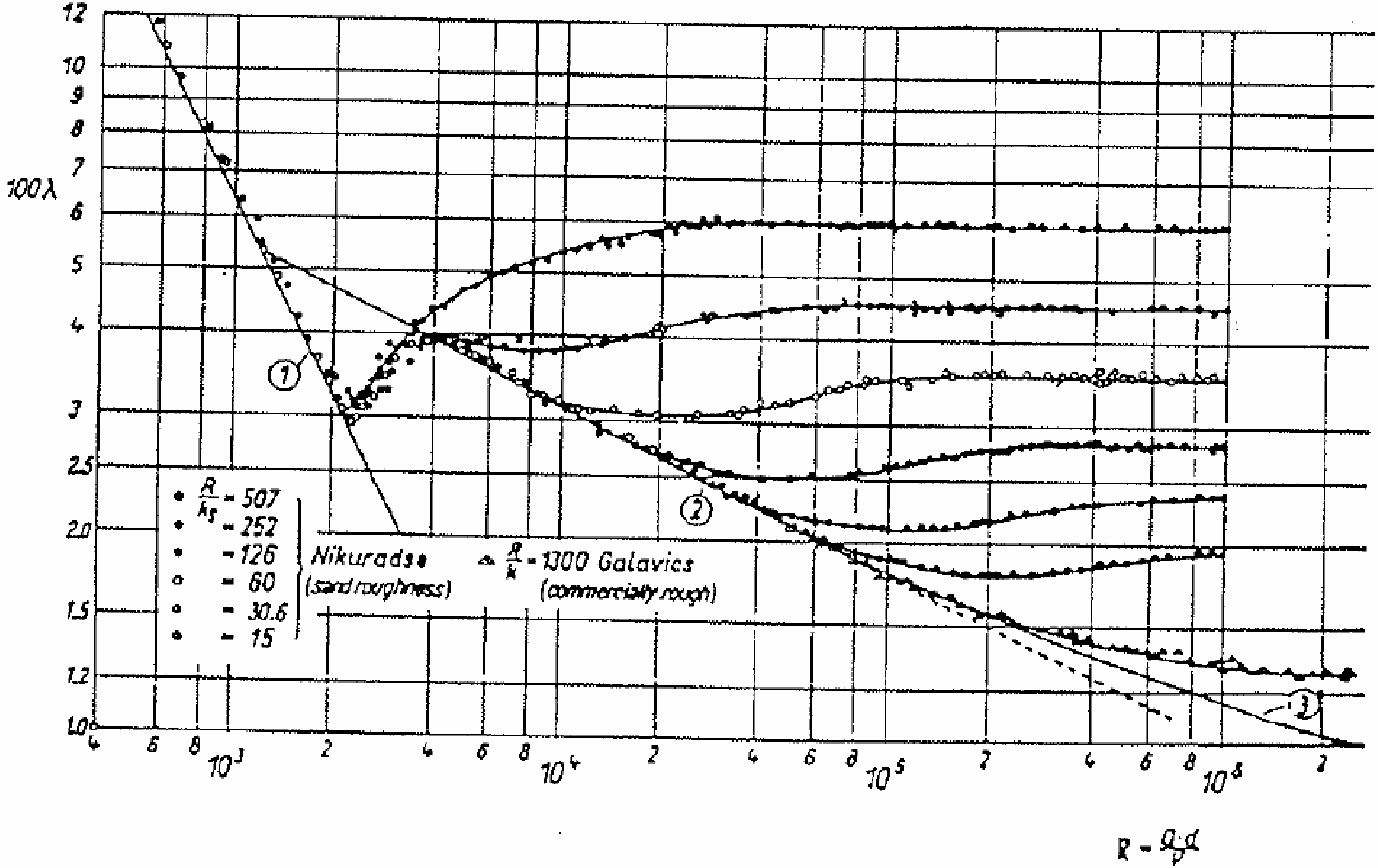

Fig. 20.18. Resistance formula for rough pipes

Curve (1) from eqn. (5.11), laminar; curve (2) from eqn. (20.5), turbulent, smooth; curve (3) from eqn. (20.30), turbulent, smooth

Worthing (1995)

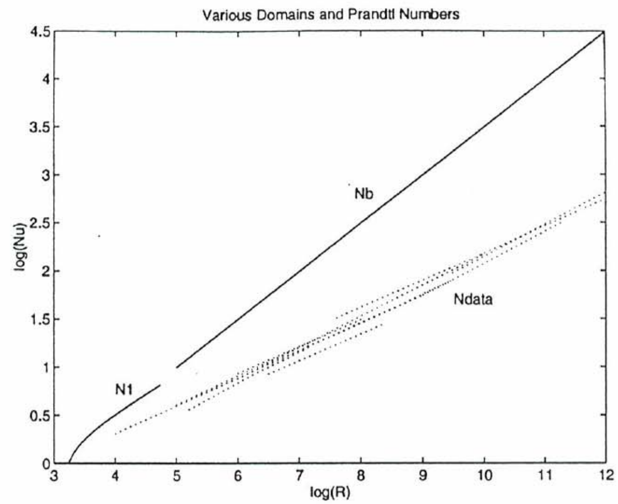

Figure 4-1: The Howard-Busse upper bound and experimental data.

N1	Howard's single-α bound (computed here)
Nb	Busse's (1969) $R \to \infty$ infinite-α bound
Ndata	Various experimental data.

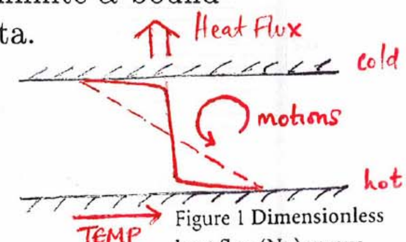

Sommeria (1999)

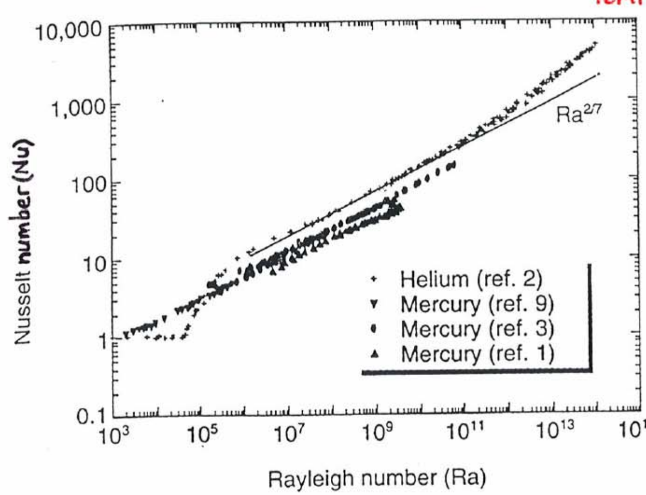

Figure 1 Dimensionless heat flux (Nu) versus temperature difference (Ra) in Rayleigh–Bénard convection. In mercury ($Pr = 0.025$), data from three experiments agree with the $Nu \propto Ra^{2/7}$ law[1,3,9]. In helium ($Pr \approx 1$) the data[2] indicate an increase in Nu, and possibly a trend towards an ultimate regime, $Nu \propto Ra^{1/2}$. Although Ra is smaller in mercury than in helium, the corresponding Reynolds numbers are comparable.

Doering & Constantin
(JFM 1998 vol 376, 263–296) PoROUS LAYER CONVECTION

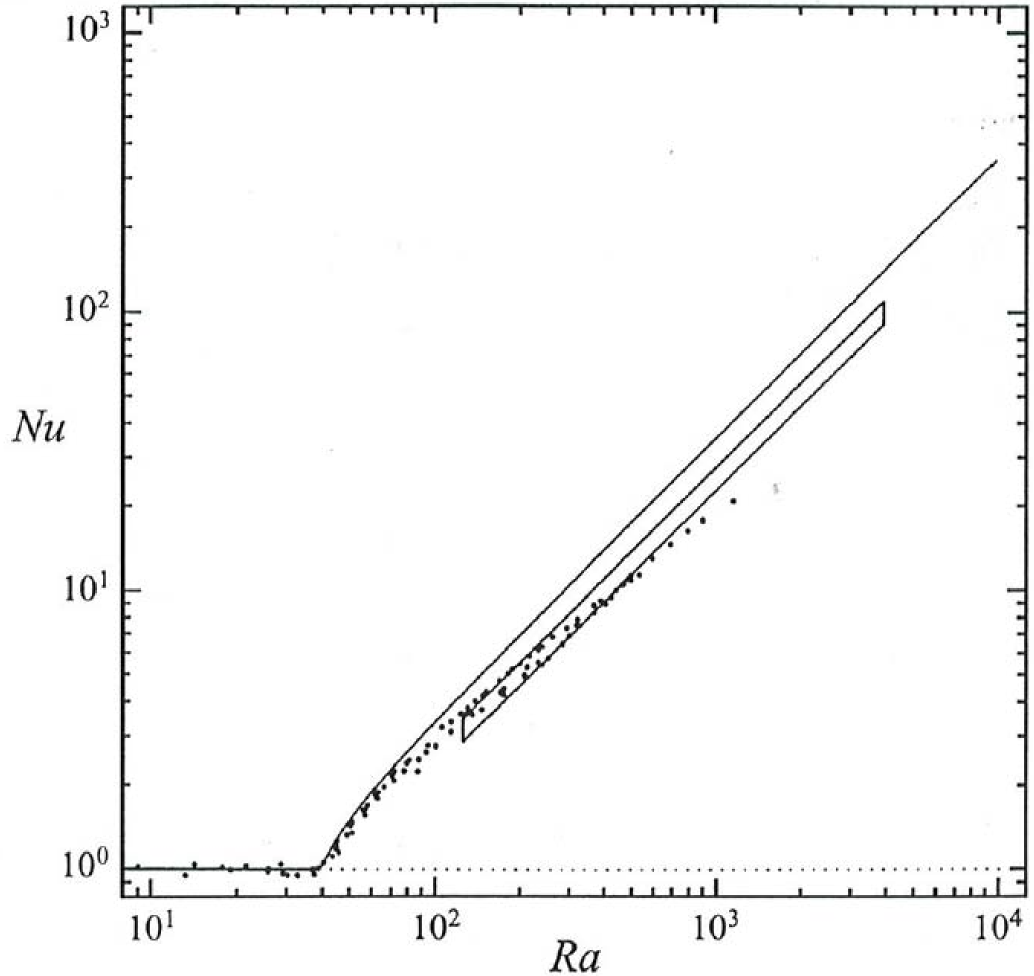

FIGURE 7. Rigorous upper bound plotted along with experimental data (see caption to
The solid curve is the lower envelope of the curves in figure 6 for all $a \in (0, 1)$.

Couette Flow with SUCTION

Doering, Spiegel & Worthing (2000)